

A Statistically-Based Approach to Feedforward Neural Network Model Selection

Andrew McInerney*

Kevin Burke†

February 22, 2023

Abstract

Feedforward neural networks (FNNs) can be viewed as non-linear regression models, where covariates enter the model through a combination of weighted summations and non-linear functions. Although these models have some similarities to the models typically used in statistical modelling, the majority of neural network research has been conducted outside of the field of statistics. This has resulted in a lack of statistically-based methodology, and, in particular, there has been little emphasis on model parsimony. Determining the input layer structure is analogous to variable selection, while the structure for the hidden layer relates to model complexity. In practice, neural network model selection is often carried out by comparing models using out-of-sample performance. However, in contrast, the construction of an associated likelihood function opens the door to information-criteria-based variable and architecture selection. A novel model selection method, which performs both input- and hidden-node selection, is proposed using the Bayesian information criterion (BIC) for FNNs. The choice of BIC over out-of-sample performance as the model selection objective function leads to an increased probability of recovering the true model, while parsimoniously achieving favourable out-of-sample performance. Simulation studies are used to evaluate and justify the proposed method, and applications on real data are investigated.

Keywords. Neural networks; Model selection; Variable selection; Information criteria.

*Department of Mathematics and Statistics, University of Limerick; andrew.mcinerney@ul.ie

†Department of Mathematics and Statistics, University of Limerick; kevin.burke@ul.ie

1 Introduction

Neural networks are a popular class of machine-learning models, which pervade modern society through their use in many artificial-intelligence-based systems (LeCun et al., 2015). Their success can be attributed to their predictive performance in an array of complex problems (Abiodun et al., 2018). Recently, neural networks have been used to perform tasks such as natural language processing (Goldberg, 2016), anomaly detection (Pang et al., 2021), and image recognition (Voulodimos et al., 2018). Feedforward neural networks (FNNs), which are a particular type of neural network, can be viewed as non-linear regression models, and have some similarities to the models traditionally used in statistical modelling (e.g., covariates enter the model through a weighted summation, and the estimation of the weights for an FNN is equivalent to the calculation of a vector-valued statistic) (Ripley, 1994; White, 1989). There was a strong interest in neural networks within the statistics community in the late 1980s and early 1990s as evidenced in the comprehensive reviews by White (1989), Ripley (1993), and Cheng and Titterton (1994). Despite this early interest, however, these models have still been historically less popular among statisticians, and the majority of neural network research has been conducted outside of the field of statistics (Breiman, 2001; Hooker and Mentch, 2021). Given this, there is a general lack of statistically-based methods, such as model and variable selection, which focus on developing parsimonious models.

Typically, the primary focus when implementing a neural network centres on model predictivity (rather than parsimony); the models are viewed as ‘black-boxes’ whose complexity is not of great concern (Efron, 2020). It is perhaps not surprising, therefore, that there is a tendency for neural networks to be highly over-parameterised, miscalibrated, and unstable (Sun et al., 2022). Nevertheless, FNNs can capture more complex covariate effects than is typical within popular (linear/additive) statistical models. Consequently, there has been renewed interest in merging statistical models and neural networks, for example, in the context of flexible distributional regression (Rügamer et al., 2020, 2021; Stasinopoulos et al., 2017) and mixed modelling (Tran et al., 2020). However, statistically-based model selection procedures are required to increase the utility of the FNN within the statistician’s toolbox.

Traditional statistical modelling is concerned with developing parsimonious models, as it is crucial for the efficient estimation of covariate effects and significance testing (Efron, 2020). Indeed, model selection (which includes variable selection) is one of the fundamental problems of statistical modelling (Fisher and Russell, 1922). It involves choosing the “best” model, from a range of candidate models, by trading pure data fit against model complexity (Anderson and Burnham, 2004). As such, there has been a substantial amount of research on model and variable selection (Miller, 2002). As noted by Heinze et al. (2018), typical approaches include significance testing combined with forward selection or backward elimination (or a combination thereof); information criteria such as AIC or BIC (Akaike, 1998; Schwarz, 1978; Anderson and Burnham, 2004); and penalised likelihood such as LASSO (Tibshirani, 1996; Fan and Lv, 2010).

In machine learning, due to the focus on model predictivity, relatively less emphasis is placed on finding a model that strikes a balance between complexity and fit. Looking at FNNs in particular, the number of hidden nodes is usually treated as a tunable hyperparameter (Bishop et al., 1995; Pontes et al., 2016). Input-node selection is not as common, as the usual consensus when fitting FNNs appears to be similar to the early opinion of Breiman (2001): “the more predictor variables, the more information”. However, there are some approaches in this direction, and a survey of variable selection techniques in machine learning can be found in Chandrashekar and Sahin (2014). In more complicated deep learning models, neural architecture searches are sometimes used, which look to automate the architecture search procedure, for example, through the use of evolutionary algorithms or reinforcement learning (Elsken et al., 2019; Wistuba et al., 2019). However, when the aforementioned approaches are implemented, the optimal model is usually determined based on its predictive performance, such as out-of-sample mean squared error, which can be calculated on a validation data set. Unlike an information criteria, out-of-sample performance does not directly take account of model complexity.

When framing an FNN statistically, there are several motivating reasons for a model selection procedure that aims to obtain a parsimonious model. For example, the estimation of parameters in a larger-than-required model results in a loss in model efficiency, which, in turn, leads to less precise estimates. Input-node selection, which is often ignored in the context of neural networks, can provide the practitioner with insights on the importance of covariates. Furthermore, eliminating irrelevant covariates can result in cheaper models by reducing potential costs associated with data collection (e.g. financial, time, energy). In this paper, we take a statistical view of neural network selection by assuming an underlying (normal) error distribution. Doing so enables us to construct a likelihood function, and, hence, carry out information-criteria-based model selection, such as the BIC (Schwarz, 1978), naturally encapsulating the parsimony in the context of a neural network. More specifically, we propose an algorithm that alternates between selecting the hidden layer complexity and the inputs with the objective of minimizing the BIC. We have found, in practice, that this leads to more parsimonious neural network models than the more usual approach of minimizing out-of-sample error, while also not compromising the out-of-sample performance itself.

The remainder of this paper is structured as follows. In Section 2, we introduce the FNN model while linking it to a normal likelihood function. Section 3 motivates and details the proposed model selection procedure. Simulation studies to investigate the performance of the proposed method, and to compare it to other approaches, are given in Section 4. In Section 5, we apply our method to real-data examples. Finally, we conclude in Section 6 with a discussion.

2 Feedforward Neural Network

Let $y = (y_1, y_2, \dots, y_n) \in \mathbb{R}^n$ be the response variable of interest for a regression-based problem, where n represents the number of observations. For the i th observation, $i = 1, \dots, n$, let $x_i = (x_{1i}, x_{2i}, \dots, x_{pi})^T$ be a vector of p covariates—the inputs to the neural network model. We assume a model of the form

$$y_i = \text{NN}(x_i) + \varepsilon_i$$

where ε_i is a random error that we assume has a $N(0, \sigma^2)$ distribution, and $\text{NN}(\cdot)$ is a neural network,

$$\text{NN}(x_i) = \gamma_0 + \sum_{k=1}^q \gamma_k \phi \left(\sum_{j=0}^p \omega_{jk} x_{ji} \right). \quad (2.1)$$

As we aim to frame FNNs as an alternative to other statistical non-linear regression models (i.e., used on small-to-medium sized tabular data sets relative to the much larger data sets seen more broadly in machine learning), and due to the universal approximation theorem (Cybenko, 1989; Hornik et al., 1989), we are restricting our attention to FNNs with a single-hidden layer. The parameters in Equation 2.1 are as follows: ω_{0k} , the bias term associated with the k th hidden node; ω_{jk} , the weight that connects the j th input node to the k th hidden node; γ_0 , the bias term associated with the output node; and γ_k , the weight that connects the k th hidden node to the output node. The function $\phi(\cdot)$ is the activation function for the hidden layer, which is often a logistic function. The number of parameters in the neural network is given by

$$K = (p + 2)q + 1. \quad (2.2)$$

A diagram of a neural network architecture with p input nodes and q hidden nodes is shown in Figure 1. In the diagram, $x_0 = 1$, $h_0 = 1$, and

$$h_k = \phi \left(\sum_{j=0}^p \omega_{jk} x_{ji} \right).$$

Given our assumption that $\varepsilon_i \sim N(0, \sigma^2)$, we then make use of the likelihood function

$$\ell(\theta) = -\frac{n}{2} \log(2\pi\sigma^2) - \frac{1}{2\sigma^2} \sum_{i=1}^n (y_i - \text{NN}(x_i))^2, \quad (2.3)$$

where $\theta = (\omega_{01}, \dots, \omega_{p1}, \dots, \omega_{0q}, \dots, \omega_{pq}, \gamma_0, \dots, \gamma_q, \sigma^2)^T$. We maximise this likelihood to obtain $\hat{\theta}$ but note that the estimates of the neural network parameters do not depend on the value of σ^2 , i.e., the residual sum of squares, $\sum_{i=1}^n (y_i - \text{NN}(x_i))^2$, can be estimated to obtain the neural network parameters. This is useful since standard neural network software (that minimises the residual sum of squares) such as `nnet` (Ripley and Venables,

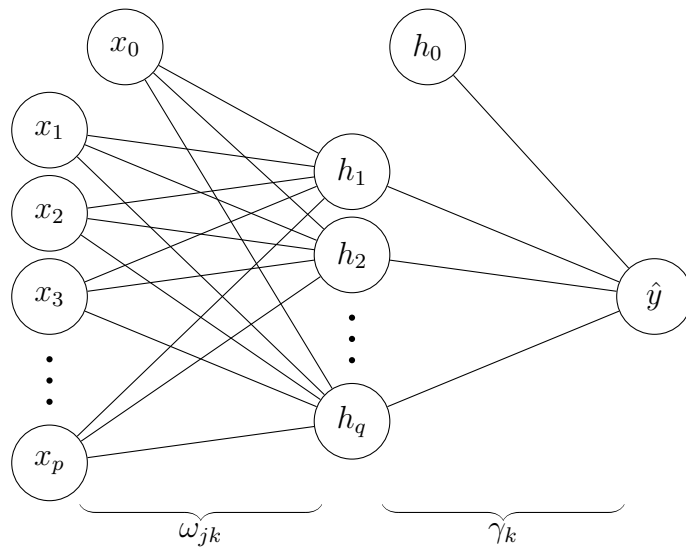


Figure 1: Neural network architecture with p input nodes and q hidden nodes.

2022) can be used to optimise the neural network followed by the estimation of σ^2 in a separate step.

The calculation of a likelihood function allows for the use of information criteria when selecting a given model, and in particular, the Bayesian information criterion (BIC) (Schwarz, 1978),

$$\text{BIC} = -2\ell(\hat{\theta}) + \log(n)(K + 1), \quad (2.4)$$

where we have $K + 1$ parameters, i.e., the K neural network parameters plus the variance parameter, σ^2 . An attractive property of the BIC is that it is “dimension-consistent”, i.e., the probability of selecting the “true” model approaches one as sample size increases (Anderson and Burnham, 2004).

3 Model Selection

To begin model selection, a set of candidate models must be considered. For the input layer, we can have up to p_{\max} inputs, where p_{\max} is the maximum number of covariates being considered, and this is often the total number of covariates available in the data under study. The input layer can contain any combination of these p_{\max} inputs. For the hidden layer, we must specify a q_{\max} value, which is the maximum number of hidden nodes to be considered; this controls the maximum level of complexity of the candidate models. We can then have between one and q_{\max} nodes in the hidden layer. From a neural network selection perspective, we aim to select a subset of $p \leq p_{\max}$ covariates to enter the input layer and to build a hidden layer of $q \leq q_{\max}$ nodes to adapt to the required complexity. To carry out these selections, we suggest a statistically-motivated procedure based on minimising the BIC, since it directly penalises complexity and is known to be

selection consistent, i.e., BIC minimisation converges to the true model asymptotically. In contrast, and more usually in machine learning applications, one could consider predictive performance, for example, the out-of-sample mean squared error. We will also consider this approach but find that it leads to significantly more complex models than the use of BIC while only marginally improving predictive performance. Whether one is aiming to minimise BIC or out-of-sample mean squared error, multiple initialisations of the neural network (from n_{init} random vectors of parameters) are required to improve the chance of finding a global maximiser of the log-likelihood surface.

3.1 Proposed Approach

We propose a stepwise procedure that starts with a hidden-node selection phase followed by an input-node selection phase. (We find that this ordering leads to improved model selection.) This is, in turn, followed by a fine-tuning phase that alternates between the hidden and input layers for further improvements. The proposed model selection procedure is detailed in Algorithm 4 (which relies on Algorithms 1–3), and a schematic diagram is provided in Figure 2. It is also described at a high level in the following paragraphs.

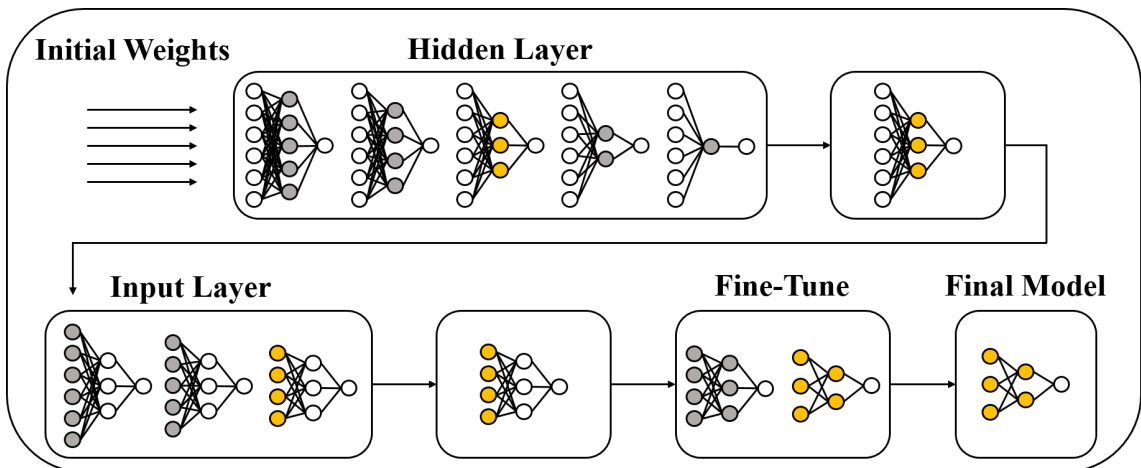


Figure 2: Model selection schematic. Nodes coloured grey are being considered in current phase. Nodes coloured gold represent optimal nodes in that phase to be brought forward to the next phase.

The procedure (Algorithm 4) is initialised with the full set of input nodes, $\mathcal{X}_{\text{full}}$, the maximum number of hidden nodes being considered, q_{max} , and the number of initialisations, n_{init} , and, as mentioned, starts with a hidden-node selection phase (Algorithm 2 with $Q = \{1, 2, \dots, q_{\text{max}} - 1\}$). For each candidate model in this phase (i.e., models with $q \in \{1, \dots, q_{\text{max}}\}$), the network optimiser is supplied with n_{init} random vectors of initial parameters, the log-likelihood function is maximised at each of these vectors, and the overall maximiser is found (see Algorithm 1). The reason for supplying the neural network with different vectors of initial parameters is due to the complex optimisation

Algorithm 1 Fit Candidate Model

Input: The set of input nodes, \mathcal{X} , the number of hidden nodes, q , and the number of initialisations n_{init} .

1. Generate n_{init} random initial weight vectors of size K , where K is given in Equation 2.2 with $p = |\mathcal{X}|$ and $|\cdot|$ is the cardinality of a set.
2. Using a neural network optimiser, maximise the log-likelihood function (Equation 2.3) for each initialisation.
3. Select the model with the maximum log-likelihood value as the candidate model.
4. Calculate the associated BIC value using Equation 2.4.

Output: A fitted neural network with its associated BIC value.

Algorithm 2 Hidden-Node Selection

Input: The set of input nodes currently included in the model, \mathcal{X} , the number of hidden nodes currently in the model, q the set of hidden-layer structures being considered, Q , and the number of initialisations n_{init} .

1. For k in Q :

Perform Algorithm 1 with the set \mathcal{X} of input nodes, k hidden nodes, and n_{init} initialisations.

If $\text{BIC}(k) \leq \text{BIC}(q)$:

Set $q = k$.

Output: The number of hidden nodes, q .

surface for neural networks that may contain several local maxima. Thus, the use of a set of initial vectors (rather than just one) aims to increase the chance of finding the global maxima; of course, this cannot be guaranteed as is often the case in more complex statistical models. Once all of the q_{max} candidate models have been fitted, the hidden-node selection phase is concluded by selecting the one whose hidden structure (i.e., number of nodes, q) minimises the BIC.

Once the hidden-node selection phase has concluded, the focus switches to the input layer (Algorithm 3); at this point, there are p_{max} inputs (i.e., the set of input nodes currently included in the model is the set of all input nodes, $\mathcal{X} = \mathcal{X}_{\text{full}}$). For the input-node selection phase, each input node is dropped in turn, with the aim of finding an input whose removal yields a lower BIC; as with the previous phase, random sets of initial parameters are used for each candidate model in the underlying likelihood optimisation. If the removal of a given input node does yield a lower BIC value, then that input node is dropped from the model (and if two or more inputs result in a lower BIC, the one

yielding the lower BIC is removed). This is repeated until no covariate, when removed from the model, results in a lower BIC, and, then, the set of included input nodes, \mathcal{X} , is returned. (Thus, in this phase, Algorithm 3 is applied with `drop = TRUE`, `add = FALSE`, and $n_{\text{steps}} = p_{\text{max}}$.)

Both the hidden layer and covariate selection phases are backward elimination procedures. Rather than stopping the algorithm after these two phases, we have found it

Algorithm 3 Input-Node Selection

Input: The set of all input nodes under consideration, $\mathcal{X}_{\text{full}}$, the set of input nodes currently included in the model, \mathcal{X} , the number of hidden nodes currently in the model, q , the switch for allowing covariates to be removed, `drop`, the switch for allowing removed covariates to be re-included, `add`, the limit on the number of iterations of the repeat step, n_{steps} , and the number of initialisations n_{init} .

1. Set $i = 0$ and $\mathcal{X}_{\text{new}} = \mathcal{X}$.

2. **Repeat:**

(a) **If** `add = TRUE`:

i. **For** c in $\mathcal{X}_{\text{full}} \setminus \mathcal{X}$:

Perform Algorithm 1 with the set $\mathcal{X} \cup \{c\}$ of input nodes, q hidden nodes, and n_{init} initialisations, where $\mathcal{X} \cup \{c\}$ is the set \mathcal{X} of input nodes with input node c added.

If $\text{BIC}(\mathcal{X} \cup \{c\}) \leq \text{BIC}(\mathcal{X}_{\text{new}})$:

Set $\mathcal{X}_{\text{new}} = \mathcal{X} \cup \{c\}$.

(b) **If** `drop = TRUE`:

i. **For** c in \mathcal{X} :

Perform Algorithm 1 with the set $\mathcal{X} \setminus \{c\}$ of input nodes, q hidden nodes, and n_{init} initialisations, where $\mathcal{X} \setminus \{c\}$ is the set \mathcal{X} of input nodes with input node c removed.

If $\text{BIC}(\mathcal{X} \setminus \{c\}) \leq \text{BIC}(\mathcal{X}_{\text{new}})$:

Set $\mathcal{X}_{\text{new}} = \mathcal{X} \setminus \{c\}$.

(c) **If** $\mathcal{X} \neq \mathcal{X}_{\text{new}}$:

Set $\mathcal{X} = \mathcal{X}_{\text{new}}$ and $i = i + 1$.

Else:

End repeat.

(d) **If** $i \geq n_{\text{steps}}$:

End repeat.

Output: The set of included input nodes, \mathcal{X} .

Algorithm 4 Model Selection

Input: The set of all input nodes, $\mathcal{X}_{\text{full}} = \{x_1, x_2, \dots, x_{p_{\text{max}}}\}$, the maximum number of hidden nodes to be considered, q_{max} , and the number of initialisations n_{init} .

1. Hidden-Node Selection:

Perform Algorithm 2 with $\mathcal{X} = \mathcal{X}_{\text{full}}$, $Q = \{1, 2, \dots, q_{\text{max}} - 1\}$, $q = q_{\text{max}}$, and $n_{\text{init}} = n_{\text{init}}$.

2. Input-Node Selection:

Perform Algorithm 3 with $\mathcal{X}_{\text{full}} = \mathcal{X}_{\text{full}}$, $\mathcal{X} = \mathcal{X}_{\text{full}}$, $q = q$, **drop** = TRUE, **add** = FALSE, $n_{\text{steps}} = p_{\text{max}}$, and $n_{\text{init}} = n_{\text{init}}$.

3. Fine Tuning:

- **Repeat:**

- (a) **Hidden Layer:**

- Perform Algorithm 2 with $\mathcal{X} = \mathcal{X}$, $Q = \{q - 1, q + 1\}$, $q = q$, and $n_{\text{init}} = n_{\text{init}}$.

- If Step 3(a) did not update the value of q :**

- End repeat.*

- (b) **Input Layer:**

- Perform Algorithm 3 with $\mathcal{X}_{\text{full}} = \{x_1, x_2, \dots, x_{p_{\text{max}}}\}$, $\mathcal{X} = \mathcal{X}$, $q = q$, **drop** = TRUE, **add** = TRUE, $n_{\text{steps}} = 1$, and $n_{\text{init}} = n_{\text{init}}$.

- If Step 3(b) did not update the value of \mathcal{X} :**

- End repeat.*

Output: The set of included input nodes, \mathcal{X} , and the number of hidden nodes, q .

* Note: The fine-tuning phase stops if either Step 3(a) or Step 3(b) does not find an improvement. This is to avoid either input-node or hidden-node selection being repeated under conditions previously considered.

fruitful to search for an improved model in a neighbourhood of the current “best” model by carrying out some further fine tuning. This is done by considering the addition or removal of one hidden node (Algorithm 2 with $Q = \{q - 1, q + 1\}$), then the further addition or removal of one input node (Algorithm 3 with **drop** = TRUE, **add** = TRUE, $n_{\text{steps}} = 1$), and these two steps are repeated alternately until no further adjustment decreases the BIC (see Step 3 in Algorithm 4). This fine-tuning stage is analogous to stepwise model selection with backward and forward steps. Note that one could apply this alternating stepwise procedure from the offset, but we have found it to be significantly more computationally efficient to focus first on the hidden and input layers (separately and in that order) before moving to the stepwise phase.

The particular order of the model selection steps described above has been chosen in order to have a higher probability in recovering the “true” model, and to have a lower computational cost (see Section 4.1 for a detailed simulation). Note that choosing the *set* of input nodes requires a more extensive search than choosing the *number* of hidden nodes. There are more candidate structures for the input layer as you can have any combination of the nodes. Therefore, it is recommended to perform hidden-node selection first, to eliminate any redundant hidden nodes and decrease the number of parameters in the model, before performing input-node selection.

4 Simulation Studies

In order to justify and evaluate the proposed model selection approach, a number of simulation studies are used:

- **Simulation 1 (Section 4.1):** In our first simulation study, we investigate the effect of the ordering of the model selection steps to justify the procedure. This includes the effect of performing input-node and hidden-node selection phases first, the improvement of including a stepwise fine-tuning step, and the performance of a procedure that only carries out iterative stepwise steps (i.e., fine tuning from the offset).
- **Simulation 2 (Section 4.2):** The second simulation study compares the performance of using the BIC as the model selection objective function versus using AIC or out-of-sample mean squared error (OOS).
- **Simulation 3 (Section 4.3):** The third simulation study investigates the performance of the proposed approach while varying the number of random initialisations.

In each simulation study, the response is generated from an FNN with known “true” architecture. The weights are generated so that there are three important inputs, x_1, x_2, x_3 , with non-zero weights, and ten unimportant inputs, x_4, \dots, x_{13} , with zero weights. The “true” hidden layer consists of $q = 3$ hidden nodes, while we set our procedure to consider a maximum of $q_{\max} = 10$ hidden nodes. In all simulation studies, we vary the sample size $n \in \{250, 500, 1000\}$ and carry out 1,000 replicates. The metrics calculated to evaluate the performance of the model selection approach are the average number of inputs with true zero weights *correctly* dropped from the model (C), the average number of hidden nodes selected (\bar{q}), the probability of choosing the correct set of inputs (PI), the probability of choosing the correct number of hidden nodes (PH), and the probability of choosing the overall true model (PT). Our proposed model selection approach is implemented in our publicly available R package `selectnn` (McInerney and Burke, 2022). The neural network function used is `nnet`, which is available from the R package of the same name (Ripley and Venables, 2022).

4.1 Simulation 1: Model Selection Approach

This simulation study aims to justify the approach of the proposed model selection procedure, i.e., a hidden-node phase, followed by an input-node phase, followed by a fine-tuning phase; here, we label this approach as H-I-F. Some other possibilities would be: to start with the input-node phase (I-H-F), to stop the procedure without fine tuning (either H-I or I-H), or to only carry out fine-tuning from the beginning (F). The objective function used for model selection is BIC, and each approach has $n_{\text{init}} = 5$ initial vectors for the optimisation procedure. (The choice of objective function and the effect of n_{init} are investigated in Sections 4.2 and 4.3, respectively.) The results of the simulation study are shown in Table 1, with boxplots for C and q displayed in Figure 3 and Figure 4, respectively.

Comparing the methods without the fine-tuning stage, H-I has a greater probability of recovering the true model versus I-H for all sample sizes. However, when looking at layerwise selection, the probability of selecting the correct structure is increased when that layer is selected in the second phase, e.g., hidden-node selection is best when it comes second. This suggests a relationship between the structure of the input and hidden layers (the probability of correctly selecting the structure of one layer increases when the other layer is more correctly specified). This is investigated further in Appendix A. Therefore, H-I is likely better than I-H due to input-node selection being a more difficult task than hidden-node selection (determining the optimal *set* of input nodes versus the optimal

Table 1: Simulation 1: model selection metrics.

n	Method	Time (s)	C (10)	\bar{q} (3)	PI	PH	PT
250	H-I	13.08	7.81	2.29	0.59	0.18	0.10
	I-H	50.37	2.53	2.85	0.01	0.44	0.01
	H-I-F	13.63	8.75	2.66	0.72	0.54	0.43
	I-H-F	52.54	4.46	2.87	0.04	0.50	0.04
	F	116.02	7.68	8.58	0.47	0.13	0.12
500	H-I	32.09	8.97	3.47	0.83	0.53	0.51
	I-H	99.74	6.44	3.14	0.43	0.87	0.40
	H-I-F	36.46	9.56	3.05	0.90	0.95	0.85
	I-H-F	103.32	7.24	3.08	0.48	0.93	0.44
	F	82.36	9.73	3.17	0.89	0.90	0.82
1000	H-I	52.73	9.98	3.02	0.99	0.98	0.97
	I-H	186.40	8.65	3.00	0.78	0.99	0.77
	H-I-F	52.66	9.99	3.00	0.99	1.00	0.99
	I-H-F	188.81	8.80	3.01	0.78	1.00	0.77
	F	168.70	9.89	3.04	0.97	0.99	0.96

Time (s), median time to completion in seconds (carried out on an Intel[®] Core[™] i5-10210U Processor). Best values for a given sample size are highlighted in **bold**.

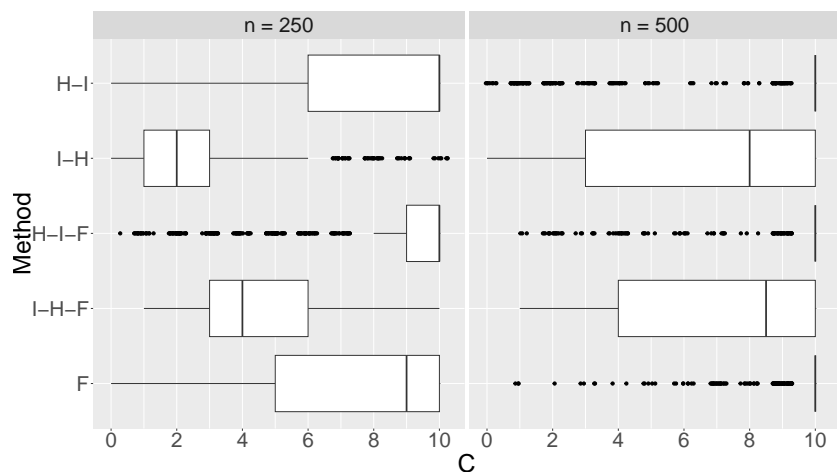


Figure 3: Simulation 1: boxplots for C (the number of inputs with true zero weights correctly dropped from the model) for each method by sample size.

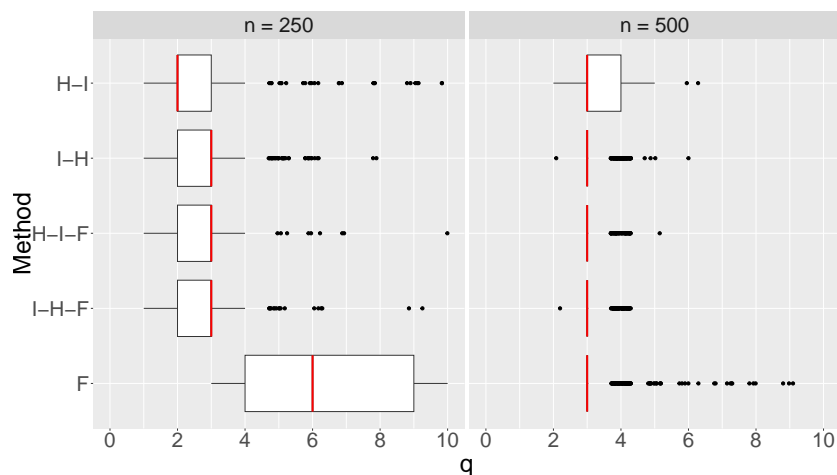


Figure 4: Simulation 1: boxplots for q (the number of hidden nodes selected) for each method by sample size. Median value highlighted in red.

number of hidden nodes), and, hence, it is favourable to perform it after hidden-node selection (given the number of hidden nodes is not substantially larger than the number of input nodes).

The relationship between the structure of both layers can be handled by incorporating a fine-tuning phase after both the H and I phases are completed. Recall that the aim of fine tuning is to search for an improved solution in a neighbourhood of the current solution, where both H and I steps are carried out alternately (and include both backward and forward selections). Indeed, we see that the addition of the fine-tuning phase improves on H-I in the smaller sample sizes (in large part due to improved hidden-layer selection), but its addition does not greatly improve on I-H. Moreover, the addition of fine tuning

only marginally adds to the computational expense. Overall, H-I-F is significantly better than I-H-F both in terms of computational expense and model selection.

One may also consider only carrying out fine-tuning steps from the offset, which we denote by F. However, this does not perform as well as H-I-F at the smallest sample size and is more computationally demanding. Since H-I yields a higher probability of recovering the *input* layer than I-H, and I-H yields a higher probability of recovering the *hidden* layer than H-I, we have also considered the following approach: run both H-I and I-H independently, then take the input layer from H-I and the hidden layer from I-H to form the model; we refer to this as [H-I*]-[I-H*]. The simulation results for this procedure are given in Appendix B but we provide an overview here. We find that the [H-I*]-[I-H*] approach outperforms both the H-I and the I-H approaches, but is more computationally expensive. The addition of a fine-tuning phase improves the model selection performance further, but the proposed H-I-F approach has very similar performance while being much less computationally demanding. Note that the various selection procedures are summarised in Table 2 and a boxplot for the computational time for each approach is provided in Appendix C.

From the above, the H-I-F approach is what we suggest as it leads to good model selection performance while also being the most computationally efficient approach.

Table 2: Simulation 1: description of model selection approaches.

Approach	Description
H-I	Hidden-node selection phase, followed by input-node selection phase (Step 1 \rightarrow Step 2).
I-H	Input-node selection phase, followed by hidden-node selection phase (Step 2 \rightarrow Step 1).
H-I-F	Hidden-node selection phase, followed by input-node selection phase, and then a fine-tuning phase (Step 1 \rightarrow Step 2 \rightarrow Step 3).
I-H-F	Input-node selection phase, followed by hidden-node selection phase, and then a fine-tuning phase (Step 2 \rightarrow Step 1 \rightarrow Step 3).
F	Fine-tuning phase only (Step 3).
[†] [H-I*]-[I-H*]	H-I approach for input-node selection, followed by I-H approach for hidden-node selection ([Step 1 \rightarrow Step 2] \rightarrow [Step 2 \rightarrow Step 1]).

Proposed approach is highlighted in **bold**.

Round brackets indicate the reordering of the steps in Algorithm 4 required to achieve the approach. Square brackets indicate a self-contained section of steps.

[†] Approach is discussed in Appendix B.

4.2 Simulation 2: Model Selection Objective Function

This simulation study aims to determine the performance of using different objective functions when carrying out model selection. In particular, it aims to determine whether the use of an information criterion can improve the ability for the model selection procedure to recover the true model; this is compared to the far more common approach in neural networks of using out-of-sample performance. Three objective functions are investigated: BIC, AIC, and out-of-sample mean squared error (OOS). The AIC approach is the same as the proposed approach in Section 3.1, swapping BIC for $AIC = -2\ell(\hat{\theta}) + 2(K + 1)$. The OOS approach follows the same procedure, but with the objective function replaced by out-of-sample mean squared error, which is calculated on an additional validation data set that is 20% the size of the training data set. A reference table for each of the model selection objective functions is given in Table 3. As before, $n_{\text{init}} = 5$ random initialisations are used. The results of the simulation study are shown in Table 4 and boxplots of C and q for the different objective functions are given in Appendix D.

Table 3: Simulation 2: description of model selection objective functions.

Objective Function	Formula
BIC (Bayesian information criterion)	$-2\ell(\hat{\theta}) + \log(n)(K + 1)$
AIC (Akaike information criterion)	$-2\ell(\hat{\theta}) + 2(K + 1)$
OOS (out-of-sample mean squared error)	$\frac{1}{\tilde{n}} \sum_{i=1}^{\tilde{n}} (\tilde{y}_i - \text{NN}(\tilde{x}_i))^2$

n , sample size; K , number of parameters in the neural network model; the OOS relates to a validation data set with \tilde{n} observations where \tilde{y}_i is the response variable and \tilde{x}_i is the covariate vector.

The results show that BIC far outperforms OOS and AIC in correctly identifying the correct FNN architecture. Using OOS as the model selection objective function never leads to correct neural network architecture being identified. This is due to the inability of the OOS to correctly identify and remove the unimportant covariates (C is always relatively low). Using AIC leads to even worse performance, and this is likely due to the weaker penalty on model complexity compared to BIC.

Given that different objective functions are being optimised, it is also of interest to compare the approaches across a range of different criteria, e.g., compute the OOS and AIC values for models selected using BIC. Table 5 contains the median AIC, BIC, and OOS values for the best model found by each approach across all simulation replicates. In addition, the median out-of-sample mean squared error evaluated on a test set is reported, which is computed on an entirely new dataset (20% the size of the training set) that the OOS-optimising procedure was not exposed to (OOS Test). Lastly, the median number of neural network parameters, K , is also shown and note that the true value is $K = 16$.

Table 4: Simulation 2: model selection metrics.

n	Method	C (10)	\bar{q} (3)	PI	PH	PT
250	AIC	2.48	11.7	0.00	0.00	0.00
	BIC	8.75	2.66	0.72	0.54	0.43
	OOS	4.51	2.79	0.04	0.28	0.01
500	AIC	2.44	11.4	0.00	0.00	0.00
	BIC	9.56	3.05	0.90	0.95	0.85
	OOS	4.61	3.91	0.03	0.36	0.00
1000	AIC	2.66	11.4	0.00	0.00	0.00
	BIC	9.99	3.00	0.99	1.00	0.99
	OOS	5.29	3.72	0.02	0.46	0.00

Best values for a given sample size are highlighted in **bold**.

As expected, in general, minimising a given objective leads to the lowest average value for that objective, e.g., a BIC-minimising procedure leads to the lowest BIC value on average among the three procedures (AIC, BIC, OOS). Interestingly however, the BIC procedure leads to very comparable OOS values to the OOS procedure (and even beats the OOS procedure in the smallest samples size); moreover, BIC-minimisation leads to the lowest OOS values on the test data. This is particularly noteworthy since this is achieved using approximately half as many parameters as the OOS-minimisation procedure. Boxplots

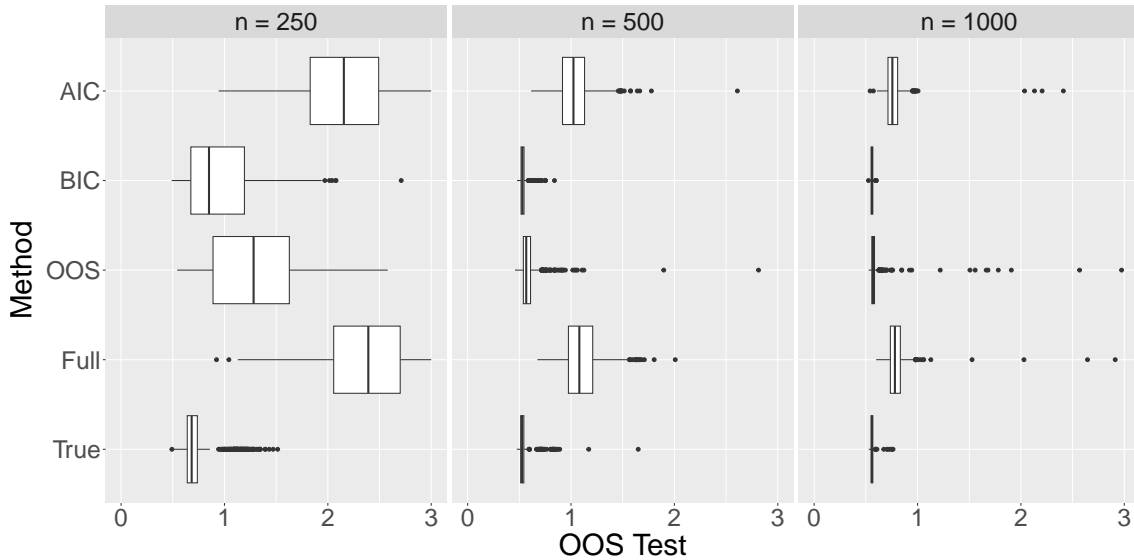


Figure 5: Simulation 2: boxplots for OOS Test for the models selected by each objective function; for comparison, the results for the true model (with inputs x_1, x_2, x_3 and $q = 3$) and the full model (with inputs x_1, x_2, \dots, x_{13} and $q = 10$).

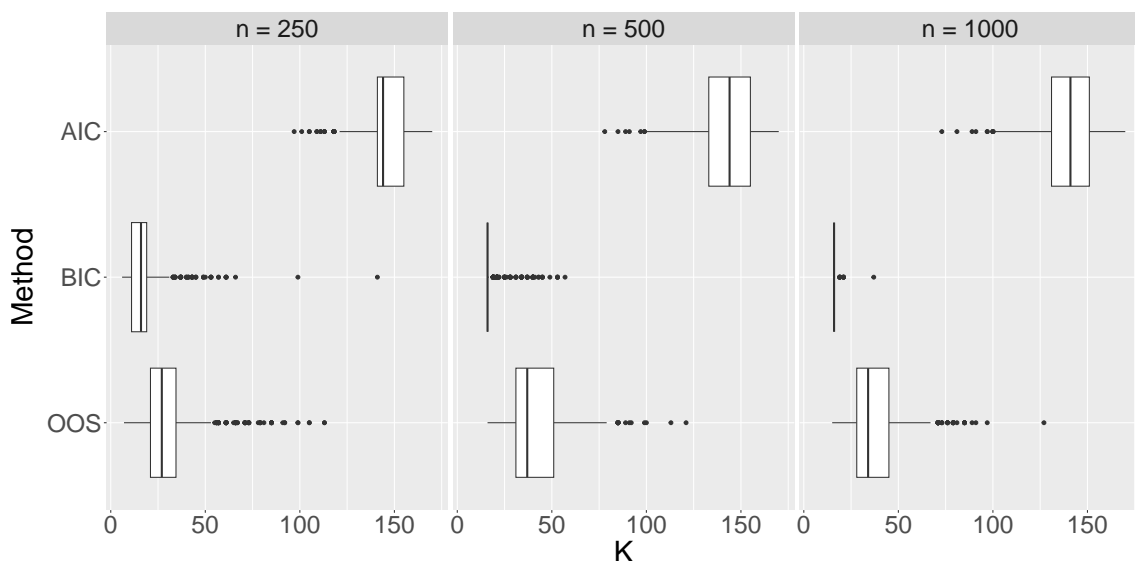


Figure 6: Simulation 2: boxplots for K (number of parameters) for the models selected by each objective function.

highlighting the values of OOS Test and K are shown in Figures 5 and 6, respectively. Figure 5 also displays the OOS Test values for the true model (inputs x_1, x_2, x_3 and $q = 3$) and the full model (inputs x_1, x_2, \dots, x_{13} and $q = 10$); this allow us to evaluate the performance of selection compared to the full model, and how close we can get to the true model. The models selected using the BIC procedure have similar performance to the true model, particularly as the sample size increases. In contrast, the models selected using AIC have worse out-of-sample performance and significantly more parameters, and the performance is similar to fitting the full model.

Table 5: Simulation 2: model performance metrics.

n	Method	AIC	BIC	OOS	OOS Test	K (16)
250	AIC	289.4	803.2	1.81	2.29	144
	BIC	572.9	646.9	0.62	0.86	16
	OOS	619.3	723.9	0.65	1.30	27
500	AIC	904.0	1507.7	0.98	1.03	144
	BIC	1078.3	1152.9	0.51	0.53	16
	OOS	1095.8	1267.2	0.50	0.57	37
1000	AIC	2002.9	2695.5	0.70	0.76	141
	BIC	2142.3	2225.9	0.50	0.56	16
	OOS	2157.6	2334.6	0.49	0.57	34

Lowest values for a given sample size are highlighted in **bold**.

4.3 Simulation 3: Number of Initialisations

Since FNNs have a complex optimisation surface (the log-likelihood function), each model fit is supplied with n_{init} random initial vectors with the aim of avoiding local maxima. Of course, larger values of n_{init} improve the chances of finding the global maximum but increase the computational expense. In the previous sections, we fixed $n_{\text{init}} = 5$, whereas, here, we vary it at $n_{\text{init}} \in \{1, 5, 10\}$ using the proposed H-I-F BIC-minimisation procedure. Plots of the probability of choosing the correct number of hidden nodes (PH), the probability of choosing the correct set of inputs (PI), and the probability of choosing the overall true model (PT) for different values of n and n_{init} are shown in Figure 7. Also, Figure 8 displays boxplots of the computational time for each scenario. The corresponding table of simulation results is given in Appendix E.

From the plots, we can clearly see the trade-off between better model selection and worse computational efficiency as n_{init} increases. We would certainly recommend $n_{\text{init}} > 1$ initial vectors since the results are poor for $n_{\text{init}} = 1$. Beyond this, the choice might be based on the computational constraints in a given practical setting, but we note, in particular, that larger values of n_{init} are more important in smaller sample sizes.

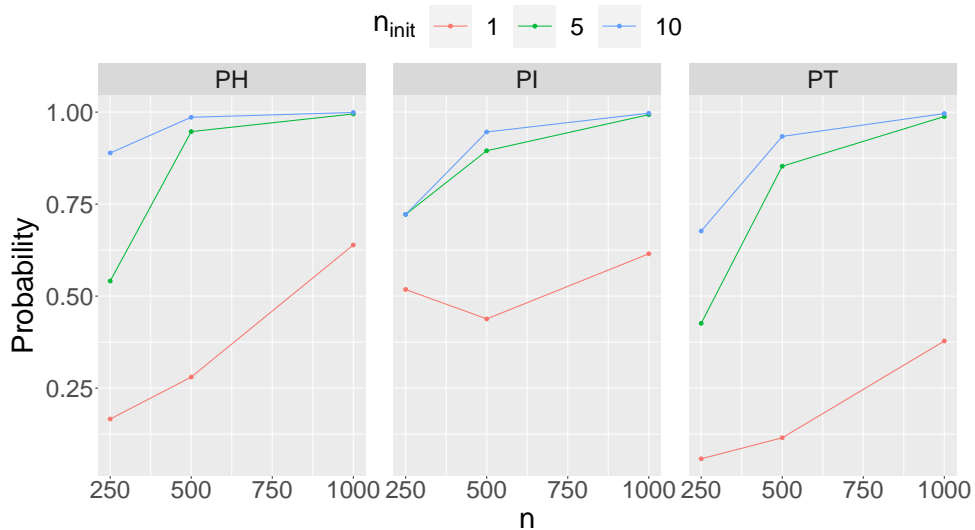


Figure 7: Simulation 3: line plots for PH (the probability of choosing the correct number of hidden nodes), PI (the probability of choosing the correct set of inputs) and PT (the probability of choosing the overall true model) for different values of n and n_{init} .

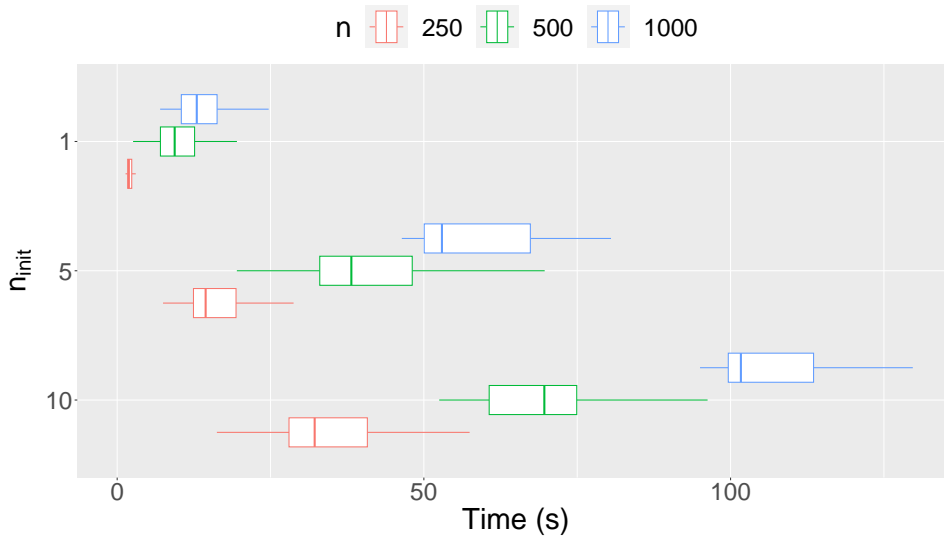


Figure 8: Simulation 3: boxplots of computational time (s) for different values of n and n_{init} .

5 Application to Data

We consider two real-data applications for our proposed model selection approach. Each dataset has been randomly split into a training set and test set with a 80%–20% split, respectively, and all variables have been rescaled (based on the training data) to be in the range $[0, 1]$. The model selection procedure was implemented with $n_{\text{init}} = 10$ and $q_{\text{max}} = 10$. For comparison purposes, the model found by our proposed model selection procedure is compared to fitting an FNN with all inputs and the maximum number of hidden nodes considered. For both models (selected and full), we report the number of input nodes (p), the number of hidden nodes (q), the total number of parameters (K), the BIC, and the out-of-sample mean squared error (OOS) computed using the test set. For the covariates that are selected, their relative importance is estimated using BIC differences (ΔBIC), which is given by

$$\Delta\text{BIC}_j = \text{BIC}_j - \text{BIC}_{\min},$$

where BIC_{\min} is the BIC for the selected model (i.e., it is the model with the minimum BIC found by our algorithm) and BIC_j is the BIC for the model with the same hidden-layer structure as this selected model but with covariate j removed; hence, the more important covariate j is, the larger the corresponding ΔBIC_j value as its removal would lead to an increased BIC_j compared to BIC_{\min} . In addition to covariate importance, simple covariate effects ($\hat{\tau}_j$) are constructed by splitting the data into two groups based on whether or not the value of j th covariate for the i th individual, x_{ji} , is above or below the empirical median value, $m_j = \text{median}(x_{j1}, x_{j2}, \dots, x_{jn})$, and computing the difference

in the average predicted response for these two groups. The corresponding equation is

$$\hat{\tau}_j = E[\text{NN}(X) \mid X_{(j)} > m_j] - E[\text{NN}(X) \mid X_{(j)} < m_j],$$

where $\text{NN}(X)$ is the output of the neural network for input covariate vector X (see Equation 2.1), $X_{(j)}$ denotes the j th covariate, and we take the conditional expected value with respect to the empirical distribution of covariates in the dataset, i.e.,

$$E[\text{NN}(X) \mid X_{(j)} > m_j] = \frac{1}{\text{card}(i \mid x_{ji} > m_j)} \sum_{i \mid x_{ji} > m_j} \text{NN}(x_i)$$

where $\text{card}(\cdot)$ is the cardinality operator. Although this metric is a simplification of the (potentially non-linear) effects captured by the neural network, and our focus is on model selection here, it is nevertheless a useful supplement to our approach that provides a high-level overview of the estimated covariate effects. The results are discussed for each dataset in Section 5.1 and 5.2.

5.1 Boston Housing Data

The Boston housing data set is available in James et al. (2022). It is a modified version of a data set that originally came from a study by Harrison and Rubinfeld (1978). It contains information relating to housing in 506 communities in the Boston area in 1970. The aim of the study was to examine the relationship between twelve explanatory variables and the median house price for each community. The explanatory variables for each community are the per capita crime rate (**crim**), the proportion of residential land zoned for lots over 25,000 sq.ft. (**zn**), the proportion of non-retail business acres per town (**indus**), the average number of rooms per dwelling (**rm**), the weighted mean of distances to five Boston employment centres (**dis**), the index of accessibility to radial highways (**rad**), the pupil-to-teacher ratio (**ptratio**), the proportion of owner-occupied units built prior to 1940 (**age**), the nitrogen oxide concentration (parts per 10 million) (**nox**), the full-value property-tax rate per \$10,000 (**tax**), an indicator of whether or not the community bounds the Charles River (**chas**), and the proportion of the population that fall into a ‘lower status’ categorisation (**lstat**). The response variable is the median value of owner-occupied homes (\$1,000s).

Our proposed procedure selects three hidden nodes and drops three covariates: **zn**, **chas** and **indus**. The selected model has 107 fewer parameters than the full model, while also having a much lower BIC value and a lower out-of-sample mean squared error. A comparison between the selected model and the full model is displayed in Table 6.

The BIC differences and covariate effects (and their associated bootstrapped confidence intervals) for the variables that remain in the model are reported in Table 7, along with a plot of the effects in Figure 9. Using ΔBIC as a measure of variable importance, we find that **rm** is the most important variable with $\Delta\text{BIC}_{\text{rm}} = 227.88$. Based on its effect ($\hat{\tau}_{\text{rm}} = 0.186$), the higher the average number of rooms per dwelling is for a community, the higher the median value of owner-occupied homes. The only other covariate with

Table 6: Boston Housing: selected versus full model comparison.

	Selected	Full
p	9	12
q	3	10
K	34	141
BIC	-983.4	-809.8
OOS	0.007	0.013

Table 7: Boston Housing: covariate effects and BIC differences.

	$\hat{\tau}_j$ (95% C.I.)	ΔBIC_j
<code>rm</code>	0.186 (0.154, 0.220)	227.88
<code>lstat</code>	-0.259 (-0.286, -0.232)	133.50
<code>dis</code>	0.115 (0.071, 0.156)	57.63
<code>crim</code>	-0.119 (-0.155, -0.084)	46.77
<code>ptratio</code>	-0.182 (-0.217, -0.149)	36.64
<code>tax</code>	-0.161 (-0.196, -0.123)	16.75
<code>age</code>	-0.135 (-0.169, -0.095)	16.57
<code>rad</code>	-0.089 (-0.127, -0.051)	14.01
<code>nox</code>	-0.160 (-0.197, -0.117)	5.78

a positive effect is `dis`, indicating that, all other things being equal, it is desirable (in terms of increased home value) to be farther from employment centres. All of the other covariates have negative effects, and, therefore, increased values of `lstat`, `crim`, `ptratio`, `tax`, `age`, `rad`, and `nox` are associated with decreased home values.

The selected model dropped three covariates (from a set of twelve possible covariates). While the underlying selection procedure cannot guarantee that this model minimises the BIC, and an exhaustive search through all sub-models is computationally expensive, we nevertheless wanted to explore how the selected model compares against a subset of alternative models (other than the full model as presented in Table 6). To this end, we fitted all twelve models that arise by dropping one of each of the covariates, twenty models where random pairs of covariates are dropped, twenty models where random triples of covariates are dropped, and twenty models where random quadruples of covariates are dropped for each hidden layer size, $q = 1, \dots, 10$. (Here, random subsets are used due to the computational expense of an exhaustive search.) Each model was allowed $n_{\text{init}} = 10$ random initialisations, mirroring that of our selection procedure. Figure 10 shows the BIC for each model where each point corresponds to a different input-layer hidden-layer combination; for comparison the model selected by our procedure is also shown. It is clear that the proposed selection procedure has indeed found a model with a BIC value that is among the lowest of the alternative models we have considered. That being said,

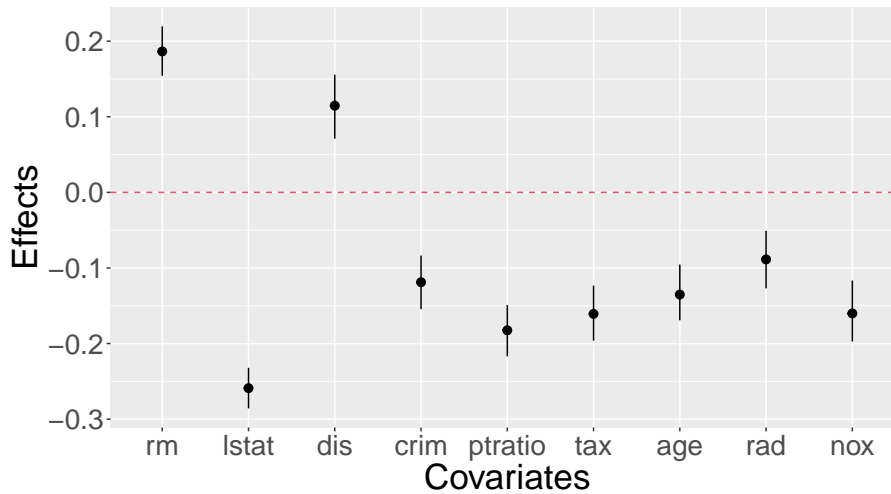


Figure 9: Boston Housing: covariate effects and their associated 95% confidence intervals.

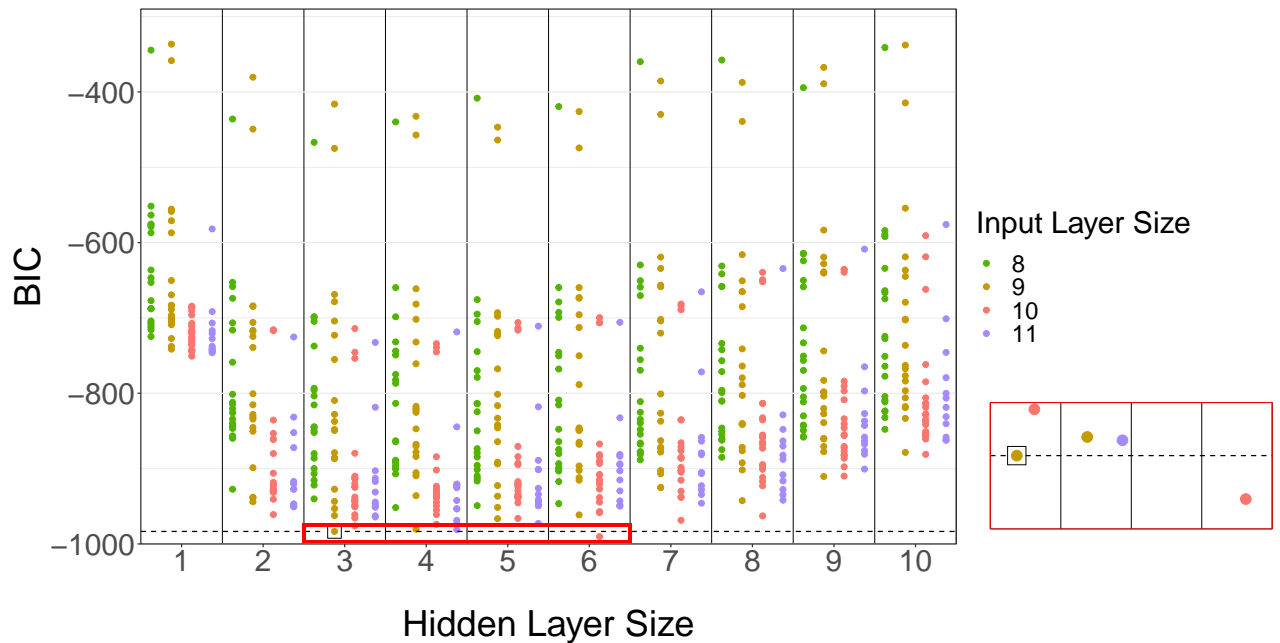


Figure 10: Boston Housing: BIC of models for different input-layer and hidden-layer combinations. Points are coloured according to the input layer size. The model selected by our procedure is enclosed in a black box and the horizontal dashed line indicates the BIC for this model. A red box is also drawn to focus on a region of interest around the selected model, and this region separately plotted to the right in a zoomed-in view.

the random search did return one model with a lower BIC value ($\Delta\text{BIC} = -6.88$). This model is more complex than the model selected by our procedure as it has $q = 6$ hidden nodes (rather than $q = 3$) and $p = 10$ input nodes (rather than $p = 9$) where it has

dropped the `zn` and `ptratio` inputs. We note that the out-of-sample prediction error for this model is equivalent to the out-of-sample prediction error for the model selected by our procedure.

5.2 Wine Quality Data Set

The wine quality data set is available on the UC Irvine Machine Learning Repository (<https://archive.ics.uci.edu/ml/datasets/wine+quality>), and was originally used by Cortez et al. (2009). The goal of the data is to examine the relationship between wine quality and some physicochemical tests. Due to the taste of red and white wine being quite different, the data is split into two separate data sets: one for white wine samples ($n = 4,898$) and another for red wine samples ($n = 1,599$). There are eleven predictor variables in total: fixed acidity (g(tartaric acid)/dm³) (`fixed`), volatile acidity (g(acetic acid)/dm³) (`vol`), citric acid (g/dm³) (`cit`), residual sugar (g/dm³) (`sugar`), chlorides (g(sodium chloride)/dm³) (`chl`), free sulfur dioxide (mg/dm³) (`fsul`), total sulfur dioxide (mg/dm³) (`tsul`), density (g/cm³) (`den`), pH (`pH`), sulphates (g(potassium sulphate)/dm³) (`sulph`), and alcohol (vol.%) (`alco`). The response variable is the quality of the wine, which was graded on a scale from zero (very bad) to ten (excellent) by a panel of expert sensory assessors.

5.2.1 Red Wine Data Set

For the red wine data, Table 8 shows that the model found by the proposed approach dropped five covariates, which are `cit`, `chl`, `sugar`, `fsul`, and `den`, and selected two hidden nodes. The selected model has a much lower BIC than the full model ($\Delta\text{BIC} = 341.7$), while having an equivalent out-of-sample performance with 114 fewer parameters; this clearly demonstrates the utility of model reduction in the context of neural networks.

Table 8: Red Wine: selected versus full model comparison.

	Selected	Full
p	6	10
q	2	10
K	17	131
BIC	-1570.3	-1228.7
OOS	0.016	0.017

The BIC differences and covariate effects (and their associated bootstrapped confidence intervals) for the variables that remain in the model are reported in Table 9, along with a plot of the effects in Figure 11. We find that `alco` is the most important variable with $\Delta\text{BIC}_{\text{alco}} = 227.01$. Based on its effect ($\hat{\tau}_{\text{alco}} = 0.137$), higher levels of alcohol volumes are associated with a greater quality of red wine. Based on ΔBIC , `sulph` and `vol` are ranked second and third for importance, respectively, but with opposite effects:

higher sulphate values are desirable for wine quality, while lower levels of volatile acidity are preferable. Lower values of total sulfur dioxide (`tsul`) and pH (`pH`) levels are also associated with higher quality red wines, and they have similar importance. The model has also selected `fixed`, but with a ΔBIC value of 1.04, this covariate has a relatively weak effect and could be removed from the model with little change to its performance.

Table 9: Red Wine: covariate effects and BIC differences.

	$\hat{\tau}_j$ (95% C.I.)	ΔBIC_j
<code>alco</code>	0.137 (0.129, 0.147)	227.01
<code>sulph</code>	0.108 (0.098, 0.118)	81.64
<code>vol</code>	-0.111 (-0.120, -0.100)	59.55
<code>tsul</code>	-0.041 (-0.052, -0.030)	10.54
<code>pH</code>	-0.015 (-0.027, -0.004)	10.42
<code>fixed</code>	0.037 (0.026, 0.048)	1.04

Similar to the analysis of the Boston housing data, we compared the BIC of the selected model to a variety of alternative models: varying the hidden layer size from one to ten, we considered the models where one of the eleven covariates was dropped and also models where we dropped two, three, four, and five covariates (twenty random subsets in each case). Figure 12 shows the BIC for each model, where, in this dataset, we find that our selection procedure (with $p = 6$ and $q = 2$) has produced the lowest BIC among all of those considered. More generally, we can see quite a strong signal in the plot that the group of models with a hidden layer size of $q = 2$ tend to have lower BIC values on average, and, for each hidden layer size, an input layer size of $p = 6$ is often best (or very close to it).

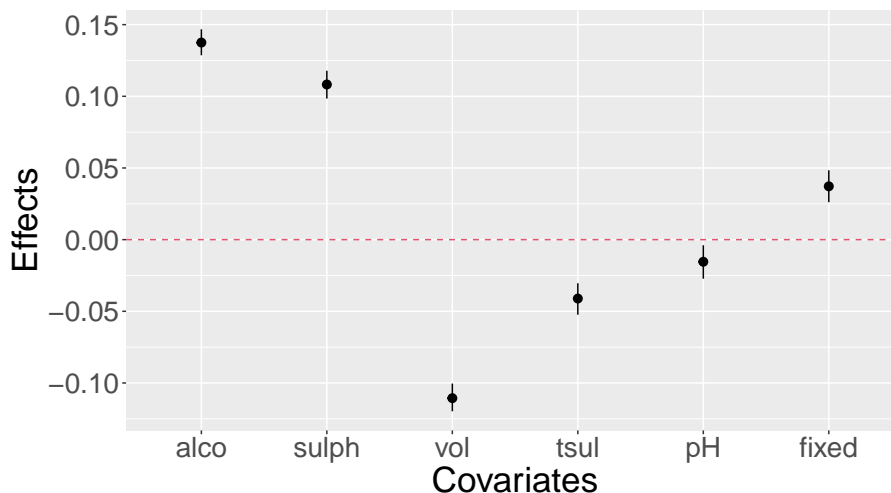


Figure 11: Red Wine: covariate effects and their associated 95% confidence intervals.

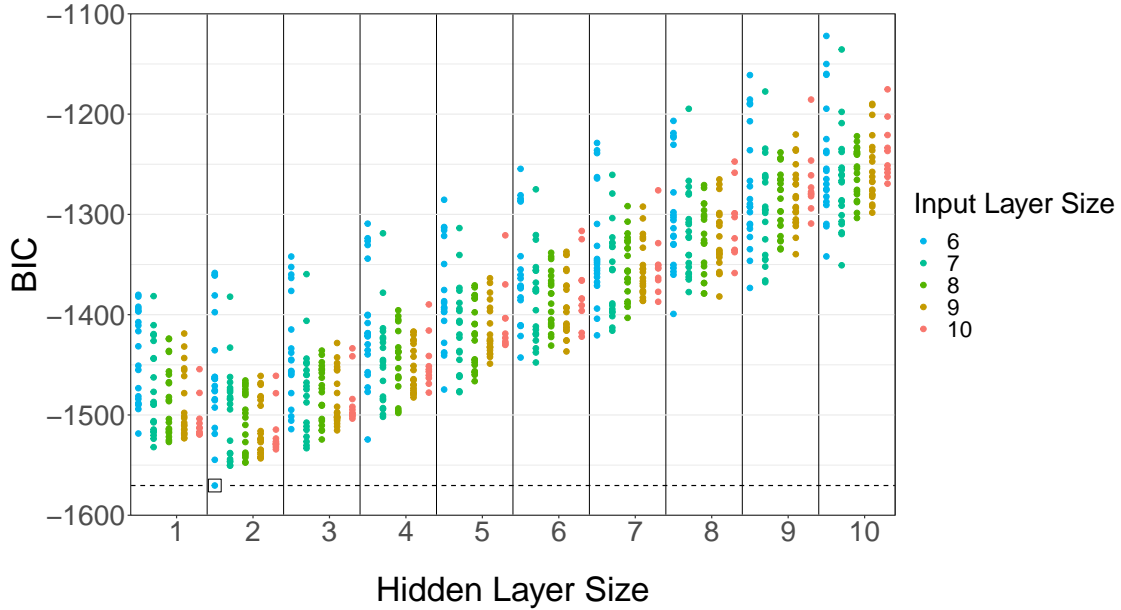


Figure 12: Red Wine: BIC of models for different input-layer and hidden-layer combinations. Points are coloured according to the input layer size. The model selected by our procedure is enclosed in a black box and the horizontal dashed line indicates the BIC for this model.

5.2.2 White Wine Data Set

For the white wine data, the proposed model selection approach identified two unimportant covariates, `chl` and `alco`, and selected a complexity of four hidden nodes. Comparing the selected model to the full model, the model selected has a lower BIC value ($\Delta\text{BIC} = 222.73$), and an equivalent out-of-sample performance while having 86 fewer weights (see Table 10).

The BIC differences and covariate effects for the selected covariates are shown in Table 11. Interestingly, it is clear that the set of features that relate to white wine quality is quite different to the set for red wine (from Section 5.2.1), and, in particular, for white

Table 10: White Wine: selected versus full model comparison.

	Selected	Full
p	9	11
q	4	10
K	45	131
BIC	-5444.5	-5221.8
OOS	0.014	0.015

Table 11: White Wine: covariate effects and BIC differences.

	$\hat{\tau}_j$ (95% C.I.)	ΔBIC_j
den	-0.084 (-0.090, -0.079)	760.38
sugar	-0.034 (-0.040, -0.028)	419.61
pH	0.029 (0.024, 0.035)	214.55
vol	-0.040 (-0.046, -0.035)	196.74
fsul	0.007 (0.001, 0.013)	136.51
fixed	-0.017 (-0.023, -0.011)	95.96
cit	-0.004 (-0.012, 0.005)	45.22
tsul	-0.047 (-0.053, -0.042)	13.45
sulph	0.005 (-0.002, 0.011)	13.36

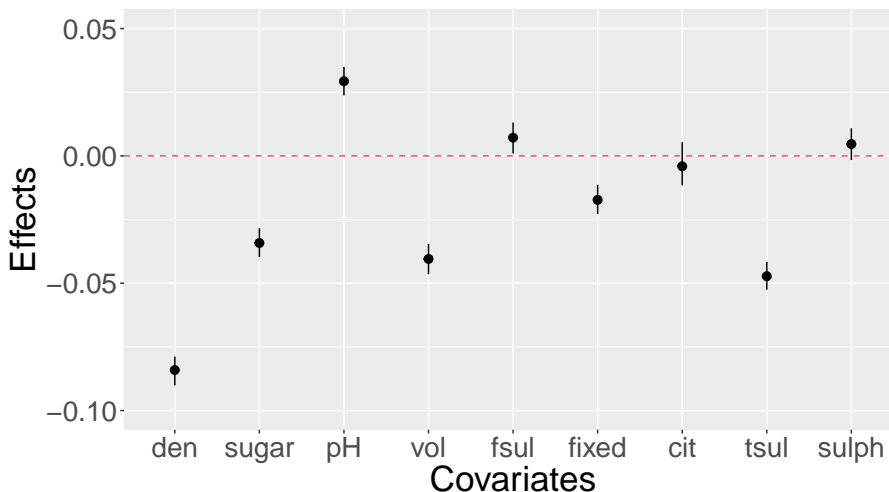


Figure 13: White Wine: covariate effects and their associated 95% confidence intervals.

wine, `alco` is not selected and `sulph` is the least important of the selected covariates (in terms of ΔBIC); these were the two most important covariates for red wine. Based on ΔBIC , we find that `den` is the most important variable with $\Delta\text{BIC} = 760.38$, with higher levels of `den` being associated with a poorer quality of white wine ($\hat{\tau}_{\text{den}} = -0.084$). The variables `sugar`, `vol`, `fixed`, `cit`, and `tsul` also have negative effects, while `pH`, `fsul`, and `sulph` have positive effects. Although some of the confidence intervals for the estimated effects contain zero (see `cit` and `sulph`), this does not imply that these covariates have no effect. As mentioned previously, these estimated effects are a simplification of the possibly non-linear effects captured by the neural network. Our focus is on model selection, but we include these estimated effects as they provide useful information alongside the set of selected inputs. As with the other datasets, we also compared our model to a set of (randomly selected) alternative models, where we found that our procedure returned the model with the lowest BIC among those considered.

6 Discussion

FNNs have become very popular in recent years and have the potential to capture more complex covariate effects than traditional statistical models. However, model selection procedures are of the utmost importance in the context of FNNs since their flexibility may increase the chance of over-fitting; indeed, the principle of parsimony is very common throughout statistical modelling more generally. Therefore, we have proposed a statistically-motivated neural network selection procedure by assuming an underlying (normal) error distribution, which then permits BIC minimisation. More specifically, our procedure involves a hidden-node selection phase, followed by an input-node (covariate) selection phase, followed by a final fine-tuning phase. We have made this procedure available in our `selectnn` package in R (McInerney and Burke, 2022).

Through extensive simulation studies, we have found that that (i) the order of selection (input versus hidden layer) is important, with respect to the probability of recovering the true model and the computational efficiency, (ii) the addition of a fine-tuning stage provides a non-negligible improvement while not significantly increasing the computational burden, (iii) using the BIC is necessary to asymptotically converge to the true model, and (iv) although the models selected using BIC have fewer parameters than those selected using out-of-sample performance, they have comparable, and sometimes improved, predictivity. We suggest that statistically-orientated model selection approaches are necessary in the application of neural networks — just as they are in the application of more traditional statistical models — and we have demonstrated the favourable performance of our proposal.

We expect that randomisation and/or divide-and-conquer throughout the selection phases would be required in more complex problems involving many covariates and/or hidden layers. Nevertheless, neural networks are still valuable in more traditional (smaller) statistical problems for which procedures such as ours will lead to more insightful outputs. Furthermore, the implementation of statistical approaches more broadly (such as uncertainty quantification and hypothesis testing) in neural network modelling will be crucial for the enhancement of these insights. This will be the direction of our future work.

Acknowledgement

This publication has emanated from research conducted with the financial support of Science Foundation Ireland under Grant number 18/CRT/6049. For the purpose of Open Access, the author has applied a CC BY public copyright licence to any Author Accepted Manuscript version arising from this submission. The second author was supported by the Confirm Smart Manufacturing Centre (<https://confirm.ie/>) funded by Science Foundation Ireland (Grant Number: 16/RC/3918).

References

- Abiodun, O. I., Jantan, A., Omolara, A. E., Dada, K. V., Mohamed, N. A., and Arshad, H. (2018). State-of-the-art in artificial neural network applications: A survey. *Heliyon*, 4(11):e00938.
- Akaike, H. (1998). *Information Theory and an Extension of the Maximum Likelihood Principle*, pages 199–213. Springer New York, New York, NY.
- Anderson, D. and Burnham, K. (2004). Model selection and multi-model inference. *Second. NY: Springer-Verlag*.
- Bishop, C. M. et al. (1995). *Neural networks for pattern recognition*, chapter 9, pages 353–354. Oxford university press.
- Breiman, L. (2001). Statistical Modeling: The Two Cultures (with comments and a rejoinder by the author). *Statistical Science*, 16(3):199 – 231.
- Chandrashekar, G. and Sahin, F. (2014). A survey on feature selection methods. *Computers & Electrical Engineering*, 40(1):16–28.
- Cheng, B. and Titterton, D. M. (1994). Neural networks: A review from a statistical perspective. *Statistical Science*, 9(1):2–30.
- Cortez, P., Cerdeira, A., Almeida, F., Matos, T., and Reis, J. (2009). Modeling wine preferences by data mining from physicochemical properties. *Decision Support Systems*, 47(4):547–553.
- Cybenko, G. (1989). Approximation by superpositions of a sigmoidal function. *Mathematics of Control, Signals and Systems*, 2(4):303–314.
- Efron, B. (2020). Prediction, estimation, and attribution. *International Statistical Review*, 88(S1):S28–S59.
- Elsken, T., Metzen, J. H., and Hutter, F. (2019). Neural architecture search: A survey. *Journal of Machine Learning Research*, 20(55):1–21.
- Fan, J. and Lv, J. (2010). A selective overview of variable selection in high dimensional feature space. *Statistica Sinica*, 20(1):101–148.
- Fisher, R. A. and Russell, E. J. (1922). On the mathematical foundations of theoretical statistics. *Philosophical Transactions of the Royal Society of London. Series A, Containing Papers of a Mathematical or Physical Character*, 222(594-604):309–368.
- Goldberg, Y. (2016). A primer on neural network models for natural language processing. *Journal of Artificial Intelligence Research*, 57:345–420.

- Harrison, D. and Rubinfeld, D. L. (1978). Hedonic housing prices and the demand for clean air. *Journal of Environmental Economics and Management*, 5(1):81–102.
- Heinze, G., Wallisch, C., and Dunkler, D. (2018). Variable selection – a review and recommendations for the practicing statistician. *Biometrical Journal*, 60(3):431–449.
- Hooker, G. and Mentch, L. (2021). Bridging breiman’s brook: From algorithmic modeling to statistical learning. *Observational Studies*, 7(1):107–125.
- Hornik, K., Stinchcombe, M., and White, H. (1989). Multilayer feedforward networks are universal approximators. *Neural Networks*, 2(5):359–366.
- James, G., Witten, D., Hastie, T., and Tibshirani, R. (2022). *ISLR2: Introduction to Statistical Learning, Second Edition*. R package version 1.3-1.
- LeCun, Y., Bengio, Y., and Hinton, G. (2015). Deep learning. *Nature*, 521(7553):436–444.
- McInerney, A. and Burke, K. (2022). *selectnn: A Statistically-Based Approach to Neural Network Model Selection*. R package version 0.0.0.9000.
- Miller, A. (2002). *Subset selection in regression*. chapman and hall/CRC.
- Pang, G., Shen, C., Cao, L., and Hengel, A. V. D. (2021). Deep learning for anomaly detection: A review. *ACM Computing Surveys (CSUR)*, 54(2):1–38.
- Pontes, F., Amorim, G., Balestrassi, P., Paiva, A., and Ferreira, J. (2016). Design of experiments and focused grid search for neural network parameter optimization. *Neurocomputing*, 186:22–34.
- Ripley, B. and Venables, W. (2022). nnet: Feed-forward neural networks and multinomial log-linear models. *R package version*, 7.3-17.
- Ripley, B. D. (1993). Statistical aspects of neural networks. In Nielsen, B. O. E., Jensen, J. L., and Kendall, W. S., editors, *Networks and Chaos: Statistical and Probabilistic Aspects*, pages 40–123. Chapman & Hall.
- Ripley, B. D. (1994). Neural networks and related methods for classification. *Journal of the Royal Statistical Society: Series B (Methodological)*, 56(3):409–437.
- Rügamer, D., Kolb, C., Fritz, C., Pfisterer, F., Kopper, P., Bischl, B., Shen, R., Bukas, C., Sousa, L. B. d. A. e., Thalmeier, D., Baumann, P., Kook, L., Klein, N., and Müller, C. L. (2021). deepregression: a flexible neural network framework for semi-structured deep distributional regression. *arXiv preprint arXiv:2104.02705*.
- Rügamer, D., Kolb, C., and Klein, N. (2020). Semi-structured deep distributional regression: Combining structured additive models and deep learning. *arXiv preprint arXiv:2002.05777*.

- Schwarz, G. (1978). Estimating the dimension of a model. *The Annals of Statistics*, 6(2):461–464.
- Stasinopoulos, M. D., Rigby, R. A., Heller, G. Z., Voudouris, V., and De Bastiani, F. (2017). *Flexible regression and smoothing: using GAMLSS in R*. CRC Press.
- Sun, Y., Song, Q., and Liang, F. (2022). Learning sparse deep neural networks with a spike-and-slab prior. *Statistics & Probability Letters*, 180:109246.
- Tibshirani, R. (1996). Regression shrinkage and selection via the lasso. *Journal of the Royal Statistical Society: Series B (Methodological)*, 58(1):267–288.
- Tran, M.-N., Nguyen, N., Nott, D., and Kohn, R. (2020). Bayesian deep net glm and glmm. *Journal of Computational and Graphical Statistics*, 29(1):97–113.
- Voulodimos, A., Doulamis, N., Doulamis, A., and Protopapadakis, E. (2018). Deep learning for computer vision: A brief review. *Computational Intelligence and Neuroscience*, 2018.
- White, H. (1989). Learning in Artificial Neural Networks: A Statistical Perspective. *Neural Computation*, 1(4):425–464.
- Wistuba, M., Rawat, A., and Pedapati, T. (2019). A survey on neural architecture search. *arXiv preprint arXiv:1905.01392*.

A Relationship between the structure of the input and hidden layer

In Simulation 1 (Section 4.1), there appears to be a relationship between the structure of one layer on the probability of selecting the correct structure for the other layer. For example, when $n = 500$, performing input-layer selection after first performing hidden-layer selection (H-I) results in a much higher probability of selecting the correct set of input nodes (PI = 0.83) in comparison to performing input-layer selection first (I-H) (PI = 0.43). This suggests that input-layer selection is improved when the hidden layer is closer to its correct structure. In order to investigate this further, we performed two simulation studies: one to explore the relationship between the input-layer structure and the probability of selecting the correct number of hidden nodes, and another to explore the relationship between the hidden-layer structure and the probability of selecting the correct set of input nodes. In each simulation study, the response is generated from an FNN with known “true” architecture containing five important inputs, x_1, x_2, \dots, x_5 , and $q = 5$ hidden nodes. Within each simulation, every scenario is implemented for 1,000 replicates, using a sample size of $n = 500$.

The aim of the first simulation study is to investigate the effect of adding additional unimportant covariates to the set of important covariates on hidden-node selection. All important covariates remain in the data, while the number of unimportant inputs, n_{unimp} , is varied from zero up to ten. The hidden-node selection step (Algorithm 2) is implemented for each replicate, with a maximum of 10 hidden nodes being considered. The probability of choosing the correct number of hidden nodes (PH) is then calculated. The results are displayed in Table 12 and Figure 14. It is clear that the more unimportant covariates that are included in the data, the lower the probability in recovering the correct hidden-layer structure.

Table 12: Probability of selecting the correct hidden-layer structure.

n_{unimp}	0	1	2	3	4	5	6	7	8	9	10
PH	0.86	0.78	0.74	0.66	0.54	0.40	0.43	0.40	0.39	0.27	0.23

n_{unimp} , the number of unimportant covariates; PH, the probability of selecting the correct number of hidden nodes.

The second simulation study aims to investigate the effect of the number of hidden nodes on input-node selection. Ten additional unimportant inputs, x_6, x_7, \dots, x_{15} , are added to the data. The number of hidden nodes is varied from one up to ten. The input-node selection step (Algorithm 3) is implemented for each replicate, and the probability of choosing the correct set of input nodes (PI) is calculated. The results are displayed in Table 13 and Figure 15. We find that closer the hidden layer is to have the correct number of hidden nodes, the greater the probability of recovering the correct set of input nodes. Both simulation studies verify that model selection for one layer is dependent on

the structure of the other layer, and, hence, justifies the use of a fine-tuning phase after performing input- and hidden-node selection.

Table 13: Probability of selecting the correct input-layer structure.

q	1	2	3	4	5	6	7	8	9	10
PI	0.01	0.53	0.59	0.58	0.71	0.60	0.63	0.66	0.63	0.58

q , the number of hidden nodes; PI, the probability of selecting the correct set of input nodes.

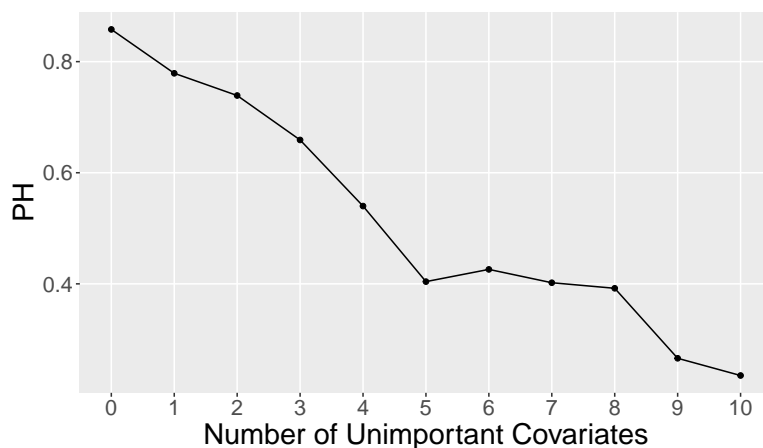


Figure 14: Number of unimportant covariates versus the probability of selecting the correct hidden-layer structure.

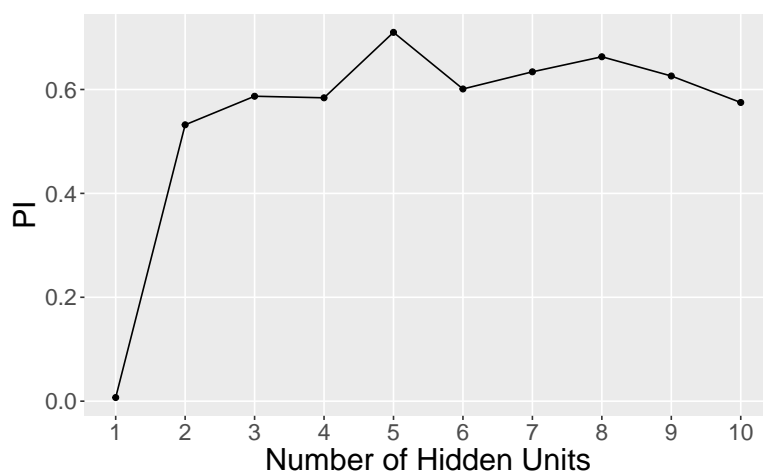


Figure 15: Number of hidden nodes versus the probability of selecting the correct input-layer structure.

B Simulation 1: Combined Approach

Two additional approaches that combine H-I selection for the input layer and I-H selection for the hidden layer are considered. The first approach consists of an input-node selection phase that first selects the number of hidden nodes, and then an independent hidden-node selection step that first selects the set of input nodes. The second approach is the same as the first, but followed by a fine-tuning phase. We refer to these approaches as [H-I*]-[I-H*] and [H-I*]-[I-H*]-F, respectively, where an asterisk denotes the layer being selected. The simulation results are displayed in Table 14.

Table 14: Model selection metrics for additional approaches.

n	Method	Time (s)	C (10)	\bar{q} (3)	PI	PH	PT
250	[H-I*]-[I-H*]	44.96	8.35	2.89	0.61	0.42	0.25
500	[H-I*]-[I-H*]	131.50	9.02	3.19	0.79	0.81	0.64
1000	[H-I*]-[I-H*]	238.15	9.97	3.00	0.98	1.00	0.98
250	[H-I*]-[I-H*]-F	45.72	8.48	2.81	0.65	0.59	0.46
500	[H-I*]-[I-H*]-F	134.73	9.30	3.04	0.85	0.96	0.82
1000	[H-I*]-[I-H*]-F	240.06	9.97	3.00	0.99	1.00	0.98

Time (s), median time to completion in seconds (carried out on an Intel[®] Core[™] i5-10210U Processor).

C Simulation 1: Boxplots of computational time for each model selection method

This section contains the boxplots associated with the computational time for the different model selection approaches, and corresponds to Table 1 in Section 4.1.

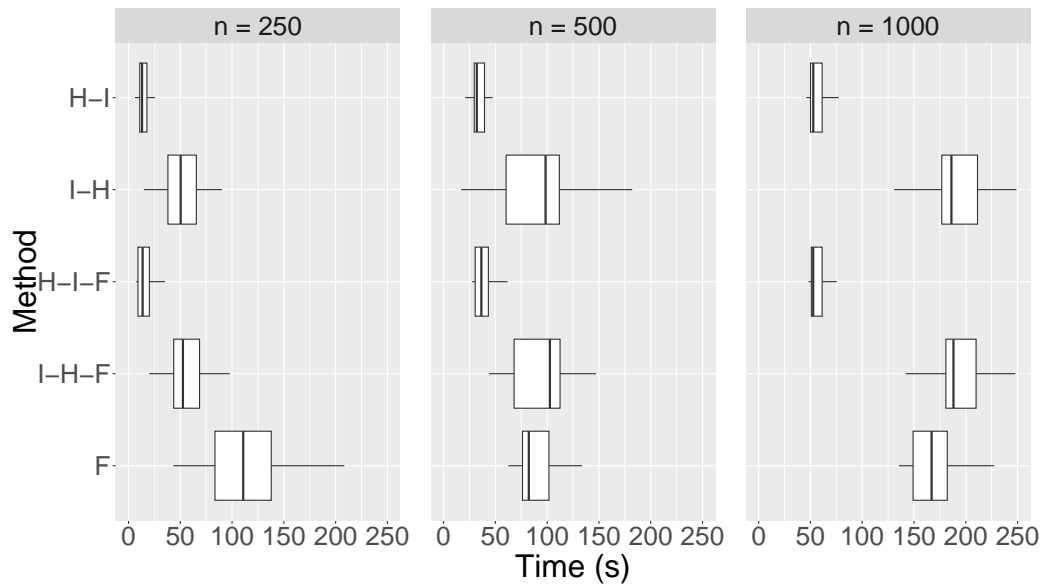


Figure 16: Simulation 1: boxplots of computational time (s) for each model selection approach and different values of n .

D Simulation 2: Boxplots of C and q for different model selection objective functions

This section contains the boxplots associated with C and q corresponding to Table 4 in Section 4.3.

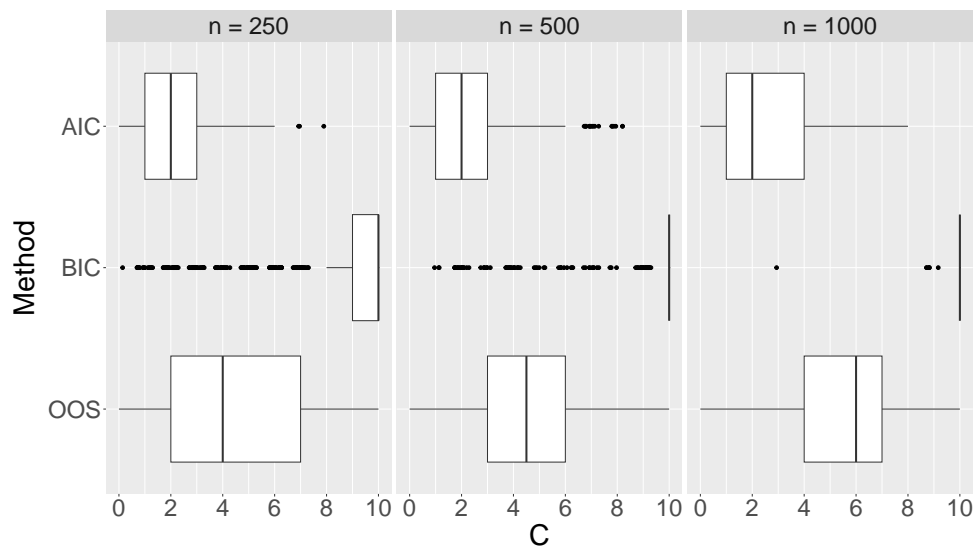


Figure 17: Simulation 2: boxplots for C (the number of inputs with true zero weights correctly dropped from the model) for the models selected by each objective function.

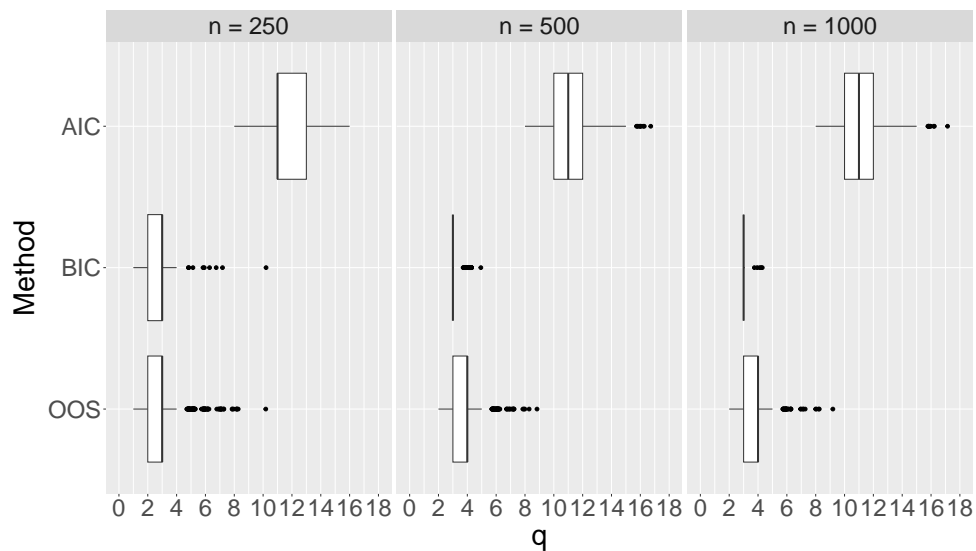


Figure 18: Simulation 2: boxplots for q (the number of hidden nodes selected) for the models selected by each objective function.

E Simulation 3: Simulation Results

This section contains the simulation results corresponding to the plots in Section 4.3.

Table 15: Simulation 3: model selection metrics.

n	n_{init}	Time (s)	C (10)	\bar{q} (3)	PI	PH	PT
250	1	1.90	8.02	2.20	0.52	0.17	0.06
	5	14.42	8.75	2.66	0.72	0.54	0.43
	10	32.30	8.87	3.05	0.72	0.89	0.68
500	1	9.37	7.35	3.82	0.44	0.28	0.12
	5	38.18	9.56	3.05	0.90	0.95	0.85
	10	70.69	9.78	3.01	0.95	0.99	0.93
1000	1	12.98	8.93	3.40	0.62	0.64	0.38
	5	54.39	9.99	3.00	0.99	1.00	0.99
	10	117.32	10.00	3.00	1.00	1.00	1.00

Time (s), median time to completion in seconds (carried out on an Intel[®] Core[™] i5-10210U Processor). Best values for a given sample size are highlighted in **bold**.